Pergamon

Int. J. Solids Structures Vol. 33, No. 29, pp. 4365–4378, 1996

0020–7683/96 $15.00 + .00

0020–7683(95)00237–5

FINITE ELEMENT PLANAR STRESS ANALYSIS

M. LAOUCET AYARI, PIXIN ZHANG and ZHIMING YE
Department of Mech. & Industrial Engineering, University of Manitoba, Winnipeg, MB, Canada R3T 2N2

(*Received* 5 *April* 1995; *in revised form* 27 *September* 1995)

Abstract—For the stress analysis of planar deformable bodies, we usually refer to either a plane stress or plane strain hypothesis. Three-dimensional analysis is required when neither hypothesis is applicable, e.g. bodies with finite thicknesses. In this paper, we derive an 'exact' solution for the plane stress problem based on a less restrictive hypothesis than $\sigma_z = 0$. By requiring the out-of-plane stress σ_z to be a harmonic function, the three-dimensional solution is obtained. In addition, we present a two-dimensional finite element for planar analysis of problems where the thickness of the body $2h$ is comparable to other characteristic dimensions. This element is presented as a substitute for classical plane stress and plane strain finite elements. The typical plane stress and plane strain state are recovered in the case where $h \to 0$ and the case $h \to \infty$, respectively. As an example for the application of such formulation, the behavior of a concrete gravity dam is investigated. Copyright © 1996 Elsevier Science Ltd.

1. INTRODUCTION

Classical plane stress and plane strain hypotheses are commonly used in the stress analysis of planar deformable bodies (see e.g. Fung (1965), Love (1927), and Timoshenko and Goodier (1954)). The plane stress state is suitable for problems involving relatively small thicknesses and free lateral boundary conditions. In the case where the thickness of a body is much larger than other characteristic dimensions, plane strain hypothesis is used. When the thickness of a body is of the same order of magnitude as other characteristic dimensions, as we often encounter in the analysis of dams constructed in structurally independent blocks, it is unclear whether plane strain hypothesis is adequate. Plane stress and plane strain assumptions are not expected to yield precise results and three-dimensional (3-D) analysis is needed. The thickness effect also appears in the evaluation of stress intensity factors in fracture mechanics (Broek (1982) and Zhou and Hsieh (1988)). Other problems arise in plasticity-based analyses where the intermediate stress and strain influence the yield locus. The difference between these two states in the evaluation of the plastic flow is remarkable, and has to be taken into account for problems with moderate thicknesses. It is thus necessary to use 3-D analyses to address many problems in engineering mechanics.

In this paper, we seek an 'exact' three-dimensional elastic solution to planar bodies with moderate thickness. This solution will involve the six compatibility equations in opposition to the classical plane stress solution which is in fact an approximation, valid only when the thickness is very small. The three-dimensional solution will not be based on the hypothesis $\sigma_z = 0$, but will, instead, require a less severe condition in which σ_z is a harmonic function, i.e.

$$\frac{\partial^2 \sigma_z}{\partial x^2} + \frac{\partial^2 \sigma_z}{\partial y^2} = 0.$$

Subsequently, we derive a planar finite element with five degrees of freedom per node to capture the thickness effect. This element not only retrieves the plane stress and plane strain solutions as limiting cases (when $h \to 0$ and $h \to \infty$), but also yields accurate results in capturing the three-dimensional solution. Numerical results will show that the maximum stress can be under-estimated by as much as 20% in the case of a cantilever beam subjected to an end point load, if either plane stress or plane strain assumption is adopted.

2. CHARACTERS OF PLANE STRESS SOLUTION (3-D ANALYSIS)

It is commonly known that, under plane strain assumption, all the equations for displacements, stresses and strains are precisely satisfied. But these equations can only be approximately satisfied under the plane stress assumption, in which we simply suppose that all the variables are independent of the z axis, which is assumed to be oriented along the thickness direction of the body, and $\sigma_z = \tau_{xz} = \tau_{yz} = 0$. The shortcoming of the plane stress assumption comes in not satisfying all the compatibility equations. The lateral strain ε_z is determined, in one aspect, as:

$$\varepsilon_z = -\frac{v}{E}(\sigma_x + \sigma_y)$$

and, in another aspect, should satisfy the compatibility equation

$$\frac{\partial^2 \varepsilon_z}{\partial x\, \partial y} = 0.$$

These two conditions are usually contradictory. Timoshenko and Goodier (1954) proposed a three-dimensional 'exact' solution of the form

$$\varphi = \varphi_0(x, y) + z^2 \varphi_1(x, y).$$

Under the assumption $\sigma_z = \tau_{xz} = \tau_{yz} = 0$, this solution satisfies all the equations of the theory of linear elasticity. In the following paragraph we show that this type of solution can be obtained without having to assume σ_z to be zero, but instead it suffices to impose the less restrictive condition

$$\nabla^2 \sigma_z = 0.$$

We seek an 'exact' three-dimensional solution under the following assumptions:

(1) $\tau_{xz} = \tau_{yz} = 0$,
(2) $\sigma_z = \sigma_z(x, y)$, and $\nabla^2 \sigma_z = 0$ (instead of the usual $\sigma_z = 0$),

where

$$\nabla^2 = \frac{\partial^2}{\partial x^2} + \frac{\partial^2}{\partial y^2} + \frac{\partial^2}{\partial z^2} \quad \text{and}$$

(3) there exists a body force potential $F(x, y)$, from which the body forces are derived as follows:

$$X = \frac{\partial F}{\partial x}, \quad Y = \frac{\partial F}{\partial y}, \quad Z = 0.$$

We depart from the compatibility equations which are the conventional requirement for the integrability of the governing equations.

$$\left.\begin{aligned} \frac{\partial^2 \varepsilon_x}{\partial y^2}+\frac{\partial^2 \varepsilon_y}{\partial x^2} &= \frac{\partial^2 \gamma_{xy}}{\partial x\,\partial y} \\ \frac{\partial^2 \varepsilon_y}{\partial z^2}+\frac{\partial^2 \varepsilon_z}{\partial y^2} &= 0 \\ \frac{\partial^2 \varepsilon_x}{\partial z^2}+\frac{\partial^2 \varepsilon_z}{\partial x^2} &= 0 \end{aligned}\right\} \quad \left.\begin{aligned} 2\frac{\partial^2 \varepsilon_x}{\partial y\,\partial z} &= \frac{\partial^2 \gamma_{xy}}{\partial x\,\partial z} \\ 2\frac{\partial^2 \varepsilon_y}{\partial x\,\partial z} &= \frac{\partial^2 \gamma_{xy}}{\partial y\,\partial z} \\ 2\frac{\partial^2 \varepsilon_z}{\partial x\,\partial y} &= -\frac{\partial^2 \gamma_{xy}}{\partial z^2} \end{aligned}\right\}. \tag{1}$$

The third equilibrium equation is identically satisfied, and the first two can be automatically satisfied if we introduce a stress function $\varphi(x, y, z)$ for which

$$\sigma_x = F+\frac{\partial^2 \varphi}{\partial y^2}, \quad \sigma_y = F+\frac{\partial^2 \varphi}{\partial x^2}, \quad \tau_{xy} = -\frac{\partial^2 \varphi}{\partial x\,\partial y}. \tag{2}$$

Introducing the generalized Hooke's law and substituting the definition of the stress function (2) into eqns (1), we obtain

$$\left.\begin{aligned} \nabla_1^2[\Theta-(1+v)F] &= 0 \\ \frac{\partial^2}{\partial x\,\partial z}[\Theta-(1+v)F] &= 0 \\ \frac{\partial^2}{\partial y\,\partial z}[\Theta-(1+v)F] &= 0 \end{aligned}\right\} \tag{3}$$

and

$$\left.\begin{aligned} \frac{\partial^2}{\partial x^2}\left[(1+v)\frac{\partial^2 \varphi}{\partial z^2}+v\Theta\right]+(1+v)\frac{\partial^2 \sigma_z}{\partial y^2} &= v\nabla^2\Theta \\ \frac{\partial^2}{\partial y^2}\left[(1+v)\frac{\partial^2 \varphi}{\partial z^2}+v\Theta\right]+(1+v)\frac{\partial^2 \sigma_z}{\partial x^2} &= v\nabla^2\Theta \\ \frac{\partial^2}{\partial x\,\partial y}\left[(1+v)\frac{\partial^2 \varphi}{\partial z^2}+v\Theta-(1+v)\sigma_z\right] &= 0 \end{aligned}\right\}, \tag{4}$$

where $\nabla_1^2 = \partial^2/\partial x^2+\partial^2/\partial y^2$ and $\Theta = \sigma_x+\sigma_y+\sigma_z$. Adding eqn (4a) to eqn (4b) yields

$$\frac{\partial^2 \Theta}{\partial z^2} = v\nabla^2\Theta. \tag{5}$$

By solving the set of eqns (3), we obtain:

$$\Theta = (1+v)F+\Theta_0+Q(z), \tag{6}$$

where $\Theta_0 = \Theta_0(x, y)$ is a harmonic function, and $Q(z)$ is an arbitrary function of z.

Equation (5) can be used to determine $Q(z)$, hence

$$\frac{d^2 Q}{dz^2} = \frac{\nu(1+\nu)}{(1-\nu)} \nabla_1^2 F. \tag{7}$$

In the above we suppose $\nabla_1^2 F = C_F$ is a constant. Because of $\nabla^2 \sigma_z = \nabla_1^2 \sigma_z = 0$ and eqn (5), eqn (4a, b, c) can be rewritten as

$$\left.\begin{aligned} \frac{\partial^2}{\partial x^2}\left[(1+\nu)\frac{\partial^2 \varphi}{\partial z^2} + \nu\Theta - (1+\nu)\sigma_z\right] &= \frac{d^2 Q}{dz^2} \\ \frac{\partial^2}{\partial y^2}\left[(1+\nu)\frac{\partial^2 \varphi}{\partial z^2} + \nu\Theta - (1+\nu)\sigma_z\right] &= \frac{d^2 Q}{dz^2} \\ \frac{\partial^2}{\partial x\,\partial y}\left[(1+\nu)\frac{\partial^2 \varphi}{\partial z^2} + \nu\Theta - (1+\nu)\sigma_z\right] &= 0 \end{aligned}\right\}, \tag{8}$$

The solution of these equations is

$$\frac{\partial^2 \varphi}{\partial z^2} = \nu\left[\frac{C_F}{2(1-\nu)}(x^2+y^2) - \frac{\Theta_0}{(1+\nu)} - F\right] + \sigma_z + ax + by + c, \tag{9}$$

where a, b and c are arbitrary functions of z. Integrating eqn (9) twice with respect to z, we find

$$\varphi = \varphi_0(x,y) + \frac{z^2}{2}\left[\frac{\nu C_F}{2(1-\nu)}(x^2+y^2) - \frac{\nu\Theta_0}{(1+\nu)} - \nu F + \sigma_z\right], \tag{10}$$

where A, B and C are functions of z, which do not contribute to planar stress components. Because we can obtain the stress components using eqn (2), therefore, A, B and C can be set to zero. Substituting eqn (10) into eqn (2), and using eqn (6) we have

$$\nabla_1^2 \varphi_0 + \frac{z^2}{2}\left[\frac{\nu(1+\nu)}{(1-\nu)} C_F\right] + 2F + \sigma_z = \Theta_0 + (1+\nu)F + Q(z). \tag{11}$$

Because the first and second terms in the right side of the above equation are independent of z, $Q(z)$ must be of the form

$$Q(z) = \frac{z^2}{2}\frac{\nu(1+\nu)}{(1-\nu)} C_F. \tag{12}$$

Applying ∇_1^2 to the two sides of eqn (11) again, we obtain

$$\nabla_1^2 \nabla_1^2 \varphi_0 = -(1-\nu)\nabla_1^2 F. \tag{13}$$

Back-substituting the solution given by eqn (10) into eqn (2) and taking into account eqn (13), the strain components are expressed in terms of Θ_0, φ_0, σ_z and F as

$$\begin{aligned} \varepsilon_x = {} & \frac{1}{E}\left[(1-\nu)F + \frac{\partial^2 \varphi_0}{\partial y^2} - \nu\left(\frac{\partial^2 \varphi_0}{\partial x^2} + \sigma_z\right)\right] \\ & + \frac{z^2}{2E}\left[\nu C_F - \nu\frac{\partial^2 F}{\partial y^2} + \nu^2\frac{\partial^2 F}{\partial x^2} - \frac{\nu}{1+\nu}\left(\frac{\partial^2 \Theta_0}{\partial y^2} - \nu\frac{\partial^2 \Theta_0}{\partial x^2}\right) + \frac{\partial^2 \sigma_z}{\partial y^2} - \nu\frac{\partial^2 \sigma_z}{\partial x^2}\right], \end{aligned} \tag{14a}$$

$$\varepsilon_y = \frac{1}{E}\left[(1-v)F + \frac{\partial^2 \varphi_0}{\partial x^2} - v\left(\frac{\partial^2 \varphi_0}{\partial y^2} + \sigma_z\right)\right]$$

$$+\frac{z^2}{2E}\left[vC_F - v\frac{\partial^2 F}{\partial x^2} + v^2\frac{\partial^2 F}{\partial y^2} - \frac{v}{1+v}\left(\frac{\partial^2 \Theta_0}{\partial x^2} - v\frac{\partial^2 \Theta_0}{\partial y^2}\right) + \frac{\partial^2 \sigma_z}{\partial x^2} - v\frac{\partial^2 \sigma_z}{\partial y^2}\right], \quad (14b)$$

$$\gamma_{xy} = -\frac{2(1+v)}{E}\left[\frac{\partial^2 \varphi_0}{\partial x \partial y} - \frac{z^2}{2}\left(v\frac{\partial^2 F}{\partial x \partial y} + \frac{v}{1+v}\frac{\partial^2 \Theta_0}{\partial x \partial y} - \frac{\partial^2 \sigma_z}{\partial x \partial y}\right)\right], \quad (14c)$$

and

$$\varepsilon_z = \frac{1}{E}[(1+v)\sigma_z - v\Theta_0 - v(1+v)F] - \frac{z^2}{2}\frac{v^2(1+v)}{E(1-v)}C_F. \quad (14d)$$

Equations (14a–d) represent the 'exact' three-dimensional solution under the less restrictive condition $\nabla^2\sigma_z = 0$. The structure of this solution will be taken as the basis for the derivation of a new finite element for the analysis of planar deformable bodies. It is important to note that this solution is truly exact only when the applied load has at most a quadratic variation along the z direction, because the in-plane stress components at any point are of form $\sigma = \sigma_0 + z^2\sigma_1$ (see eqns (14a–d)). This issue is not of practical concern for the purpose of this contribution, as we intend to capture the thickness effect and the load distribution in 'z' direction will be considered to be constant per unit thickness (similar to the classical plane stress problem).

3. DISPLACEMENT MODES

The analyses of the previous section shows that the stress function consists of two terms: the first term is the traditional Airy's stress function, which is independent of the coordinate z; the second term, a quadratic term in z, which vanishes when the thickness $2h \to 0$. The structure of the planar strain components ε_x, ε_y and γ_{xy} is the same. This suggests the planar displacement components of the new element to have the following form

$$\left.\begin{aligned} u &= u_0(x,y) + z^2 u_1(x,y) \\ v &= v_0(x,y) + z^2 v_1(x,y) \end{aligned}\right\}. \quad (15)$$

It is worth noting that one of the necessary conditions for obtaining solution (10) is $\nabla^2\sigma_z = 0$, instead of $\sigma_z = 0$. This means that the lateral stress is not necessarily zero through the thickness. Also, eqn (14d) shows that, once $C_F = 0$, the lateral strain ε_z is uniform along the thickness direction z, therefore the displacement in the z-direction can be approximated by:

$$w = z w_0(x,y). \quad (16)$$

With the above displacement modes we obtain the following expressions of the strain components:

$$\varepsilon_x = \frac{\partial u_0}{\partial x} + z^2\frac{\partial u_1}{\partial x}, \quad \gamma_{xy} = \left(\frac{\partial u_0}{\partial y} + \frac{\partial v_0}{\partial x}\right) + z^2\left(\frac{\partial u_1}{\partial y} + \frac{\partial v_1}{\partial x}\right),$$

$$\varepsilon_y = \frac{\partial v_0}{\partial y} + z^2\frac{\partial v_1}{\partial y}, \quad \gamma_{xz} = z\left(\frac{\partial w_0}{\partial x} + 2u_1\right), \varepsilon_z = w_0 \quad \text{and} \quad \gamma_{yz} = z\left(\frac{\partial w_0}{\partial y} + 2v_1\right). \quad (17)$$

Non-zero out of plane shear strains γ_{xz} and γ_{yz} appear in the above formulae. Later on it will be seen that they are introduced in the form of a penalty term in the variational formula of the potential energy, and their numerical values are negligible.

4. FINITE ELEMENT APPROXIMATION

The isoparametric element formulation is used in the discretization process. There are five degrees of freedom at each node. For an arbitrary node i these degrees of freedom are:

$$\boldsymbol{\delta}_i^{\mathrm{T}} = \{u_{0i} \quad v_{0i} \quad w_{0i} \quad u_{1i} \quad v_{1i}\}. \tag{18}$$

The element can be either the 3-node triangle, 6-node triangle, 4-node quadrilateral or 8-node quadrilateral serendipity elements. The nodal displacement array of an *n-node* element is given by

$$\boldsymbol{\delta}^{\mathrm{T}} = \{\boldsymbol{\delta}_1^{\mathrm{T}} \quad \boldsymbol{\delta}_2^{\mathrm{T}} \quad \ldots \quad \boldsymbol{\delta}_n^{\mathrm{T}}\}. \tag{19}$$

The values of u_0, v_0, w_0, u_1 and v_1 within an element are interpolated using the usual shape functions:

$$u_0 = \sum_{i=1}^{n} N_i u_{0i}, \quad v_0 = \sum_{i=1}^{n} N_i v_{0i}, \quad w_0 = \sum_{i=1}^{n} N_i w_{0i}, \quad u_1 = \sum_{i=1}^{n} N_i u_{1i} \quad \text{and} \quad v_1 = \sum_{i=1}^{n} N_i v_{1i}, \tag{20}$$

where N_i, $i = 1, 2, \ldots, n$ are the shape functions. The strain array

$$\boldsymbol{\varepsilon}^{\mathrm{T}} = \{\varepsilon_x \quad \varepsilon_y \quad \gamma_{xy} \quad \varepsilon_z \quad \gamma_{xz} \quad \gamma_{yz}\}$$

can be arranged as:

$$\varepsilon^{\mathrm{T}} = \{\varepsilon_0^{\mathrm{T}} + z^2\varepsilon_1^{\mathrm{T}} \quad z\varepsilon_2^{\mathrm{T}}\}, \tag{21}$$

where ε_0, ε_1 and ε_2 are defined by:

$$\boldsymbol{\varepsilon}_0 = \begin{Bmatrix} \dfrac{\partial u_0}{\partial x} \\ \dfrac{\partial v_0}{\partial y} \\ \dfrac{\partial u_0}{\partial y} + \dfrac{\partial v_0}{\partial x} \\ w_0 \end{Bmatrix}, \quad \boldsymbol{\varepsilon}_1 = \begin{Bmatrix} \dfrac{\partial u_1}{\partial x} \\ \dfrac{\partial v_1}{\partial y} \\ \dfrac{\partial u_1}{\partial y} + \dfrac{\partial v_1}{\partial x} \\ 0 \end{Bmatrix}, \quad \boldsymbol{\varepsilon}_2 = \begin{Bmatrix} \dfrac{\partial w_0}{\partial x} + 2u_1 \\ \dfrac{\partial w_0}{\partial_y} + 2v_1 \end{Bmatrix}. \tag{22}$$

By virtue of eqn (20) and eqn (22), $\boldsymbol{\varepsilon}_0$, $\boldsymbol{\varepsilon}_1$ and $\boldsymbol{\varepsilon}_2$ are related to the nodal displacement array δ through $\mathbf{B}_0$, $\mathbf{B}_1$ and $\mathbf{B}_2$ in the following form,

$$\boldsymbol{\varepsilon}_0 = \mathbf{B}_0\boldsymbol{\delta}, \quad \boldsymbol{\varepsilon}_1 = \mathbf{B}_1\boldsymbol{\delta}, \quad \boldsymbol{\varepsilon}_2 = \mathbf{B}_2\boldsymbol{\delta}, \tag{23}$$

where

$$\mathbf{B}_0 = [\mathbf{B}_0^1 \quad \ldots \quad \mathbf{B}_0^n],$$

$$\mathbf{B}_0^i = \begin{bmatrix} \frac{\partial N_i}{\partial x} & 0 & 0 & 0 & 0 \\ 0 & \frac{\partial N_i}{\partial y} & 0 & 0 & 0 \\ \frac{\partial N_i}{\partial y} & \frac{\partial N_i}{\partial x} & 0 & 0 & 0 \\ 0 & 0 & N_i & 0 & 0 \end{bmatrix}; \tag{24}$$

$$\mathbf{B}_1 = [\mathbf{B}_1^1 \quad \ldots \quad \mathbf{B}_1^n],$$

$$\mathbf{B}_1^i = \begin{bmatrix} 0 & 0 & 0 & \frac{\partial N_i}{\partial x} & 0 \\ 0 & 0 & 0 & 0 & \frac{\partial N_i}{\partial y} \\ 0 & 0 & 0 & \frac{\partial N_i}{\partial y} & \frac{\partial N_i}{\partial x} \\ 0 & 0 & 0 & 0 & 0 \end{bmatrix}; \tag{25}$$

and

$$\mathbf{B}_2 = [\mathbf{B}_2^1 \quad \ldots \quad \mathbf{B}_2^n],$$

$$\mathbf{B}_2^i = \begin{bmatrix} 0 & 0 & \frac{\partial N_i}{\partial x} & 2N_i & 0 \\ 0 & 0 & \frac{\partial N_i}{\partial y} & 0 & 2N_i \end{bmatrix}. \tag{26}$$

The stress array $\boldsymbol{\sigma}^{\mathrm{T}} = \{\sigma_x \quad \sigma_y \quad \tau_{xy} \quad \sigma_z \quad \tau_{xz} \quad \tau_{yz}\}$ and the strain array satisfy the elastic relation:

$$\boldsymbol{\sigma} = \mathbf{D}\boldsymbol{\varepsilon}. \tag{27}$$

The elasticity matrix $\mathbf{D}$, written in block form, is given by:

$$\mathbf{D} = \begin{bmatrix} \mathbf{D}_1 & 0 \\ 0 & \mathbf{D}_2 \end{bmatrix}, \tag{28}$$

where

$$\mathbf{D}_1 = \frac{E(1-\nu)}{(1+\nu)(1-2\nu)} \begin{bmatrix} 1 & \frac{\nu}{(1-\nu)} & 0 & \frac{\nu}{(1-\nu)} \\ \frac{\nu}{(1-\nu)} & 1 & 0 & \frac{\nu}{(1-\nu)} \\ 0 & 0 & \frac{(1-2\nu)}{2(1-\nu)} & 0 \\ \frac{\nu}{(1-\nu)} & \frac{\nu}{(1-\nu)} & 0 & 1 \end{bmatrix}$$

and $\mathbf{D}_2 = G\mathbf{I}$, where $\mathbf{I}$ is a 2×2 identity matrix.

5. MINIMUM POTENTIAL ENERGY PRINCIPLE AND STIFFNESS MATRIX

Following the standard form of the displacement based finite element method, we derive the stiffness matrix and nodal force vector using the minimum potential energy principle. The potential energy of the system can be written as:

$$\Pi = \int_V \frac{1}{2}\boldsymbol{\sigma}^{\mathrm{T}}\boldsymbol{\varepsilon}\,\mathrm{d}v - \int_V \mathbf{f}^{\mathrm{T}}\mathbf{u}\,\mathrm{d}v - \int_S \mathbf{t}^{\mathrm{T}}\mathbf{u}\,\mathrm{d}s, \tag{29}$$

where **f** and **t** are the body force vector and the traction vector acting on the boundary respectively, and **u** is the displacement vector. The in-plane displacements are thus given by

$$\mathbf{u} = \begin{Bmatrix} u \\ v \end{Bmatrix} = \begin{Bmatrix} u_0 + z^2 u_1 \\ v_0 + z^2 v_1 \end{Bmatrix} = (\mathbf{N}_0 + z^2\mathbf{N}_1)\,\boldsymbol{\delta}. \tag{30}$$

By using eqns (21), (23), (27) and (29), the potential energy is expressed in terms of strains and nodal displacement array as

$$\Pi = \int_V \frac{1}{2}(\boldsymbol{\varepsilon}_0^{\mathrm{T}} + z^2\boldsymbol{\varepsilon}_1^{\mathrm{T}} z\boldsymbol{\varepsilon}_2^{\mathrm{T}})D(\boldsymbol{\varepsilon}_0 + z^2\boldsymbol{\varepsilon}_1 z\boldsymbol{\varepsilon}_2)\,\mathrm{d}z\,\mathrm{d}\Omega - \int_V \boldsymbol{\delta}^{\mathrm{T}}(\mathbf{N}_0^{\mathrm{T}} + z^2\mathbf{N}_1^{\mathrm{T}})\mathbf{f}\,\mathrm{d}z\,\mathrm{d}\Omega$$

$$- \int_S \boldsymbol{\delta}^{\mathrm{T}}(\mathbf{N}_0^{\mathrm{T}} + z^2\mathbf{N}_1^{\mathrm{T}})t\,\mathrm{d}z\,\mathrm{d}\Gamma, \tag{31}$$

where Ω is the center plane area with the boundary line Γ. Equation (31) can be explicitly integrated along the z-direction. According to the stationary condition of the potential energy, we obtain the finite element discrete system of equations:

$$(\Sigma\mathbf{K}_e)\,\boldsymbol{\delta} = \mathbf{F}, \tag{32}$$

with the element stiffness matrix $\mathbf{K}_e$, written in a standard form as:

$$\mathbf{K}_e = 2h\int_{\Omega_e}\left[\mathbf{B}_0^{\mathrm{T}}\mathbf{D}_1\mathbf{B}_0 + \frac{h^2}{3}(\mathbf{B}_0^{\mathrm{T}}\mathbf{D}_1\mathbf{B}_1 + \mathbf{B}_1^{\mathrm{T}}\mathbf{D}_1\mathbf{B}_0 + \mathbf{B}_2^{\mathrm{T}}G\mathbf{B}_2) + \frac{h^4}{5}\mathbf{B}_1^{\mathrm{T}}\mathbf{D}_1\mathbf{B}_1\right]\mathrm{d}\Omega \tag{33}$$

and the equivalent nodal force vector **F**

$$\mathbf{F} = \Sigma 2h\int_{\Omega_e}\left(\mathbf{N}_0^{\mathrm{T}} + \frac{h^2}{3}\mathbf{N}_1^{\mathrm{T}}\right)\mathbf{f}\,\mathrm{d}\Omega + \Sigma 2h\int_{\Gamma_e}\left(\mathbf{N}_0^{\mathrm{T}} + \frac{h^2}{3}\mathbf{N}_1^{\mathrm{T}}\right)\mathbf{t}\,\mathrm{d}\Gamma, \tag{34}$$

where **t** is also assumed to be independent of z.

The detailed matrix expression of the element stiffness is given in the Appendix. In the expression given by eqn (33), the term $\mathbf{B}_0^{\mathrm{T}}\mathbf{D}_1\mathbf{B}_1 + \mathbf{B}_1^{\mathrm{T}}\mathbf{D}_1\mathbf{B}_0$ represents the coupling between the first and second terms of the displacement mode definition given by eqn (15). This coupling becomes weaker when the thickness decreases, and the plane stress condition recovers. $\mathbf{B}_2^{\mathrm{T}}G\mathbf{B}_2$ corresponds to the deformation energy caused by the lateral shear strains γ_{xz} and γ_{yz}. It stands as a penalty term to enforce the important relations between u_1, v_1 and w_0 as it will be shown in Section 7.

On the edge boundary the prescribed displacements are supposed to be constant over the thickness, u_0 and v_0 should satisfy these displacement boundary conditions, and, therefore, u_0 and v_0 on the edge are simply made zero.

6. NUMERICAL RESULTS

The cantilever beam shown in Fig. 1 is analyzed using the new element. A 20×2 mesh, with a 2×2 Gaussian integration, is used to discretize the beam. The thickness $2h$ of the beam is varied to examine the behavior of the new element. The deflection at the tip is depicted against h in Fig. 2. The same model is independently analyzed using plane stress, plane strain and three-dimensional 20-node elements. It can be seen from Fig. 2 that for the limit case when $h \to 0$ the solution coincides with the plane stress one, while when $h \to \infty$, the solution coincides with the plane strain one. In the center plane (i.e. $z = 0$), the solution is very close to the three-dimensional analysis. In the range of $0 < h/a < 1$, the plane stress solution is a good approximation; and for $h/a > 100$ the plane strain hypothesis is considered to be adequate. The variation of maximum stress vs the thickness $2h$ is shown in Fig. 3. Again, it is noted that in the range $1 < h/a < 100$, the thickness has a significant influence on the maximum stress. When the thickness of the cantilever beam is about twelve times the depth of the beam, the maximum bending stress at the central plane reaches a value 20% larger than the one predicted by either plane stress or plane strain. The result signals that the plane stress or plane strain states should be adopted with care in two

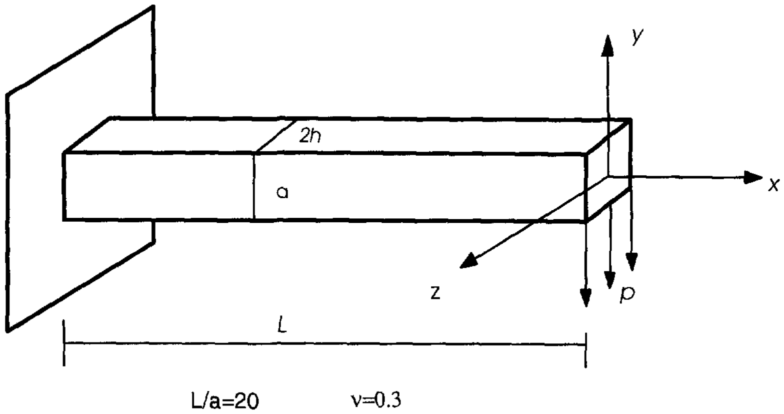

Fig. 1. Cantilever beam ($\nu = 0.3$).

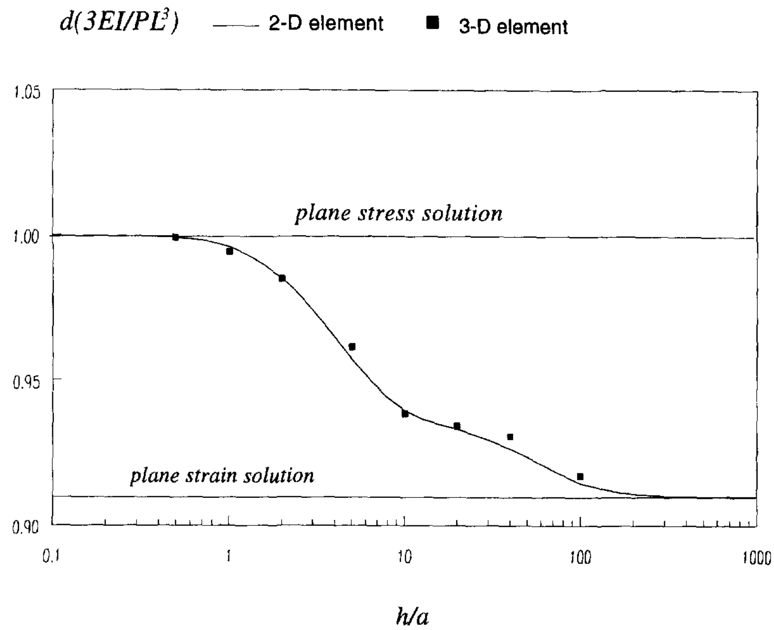

Fig. 2. The influence of thickness on the end deflection d.

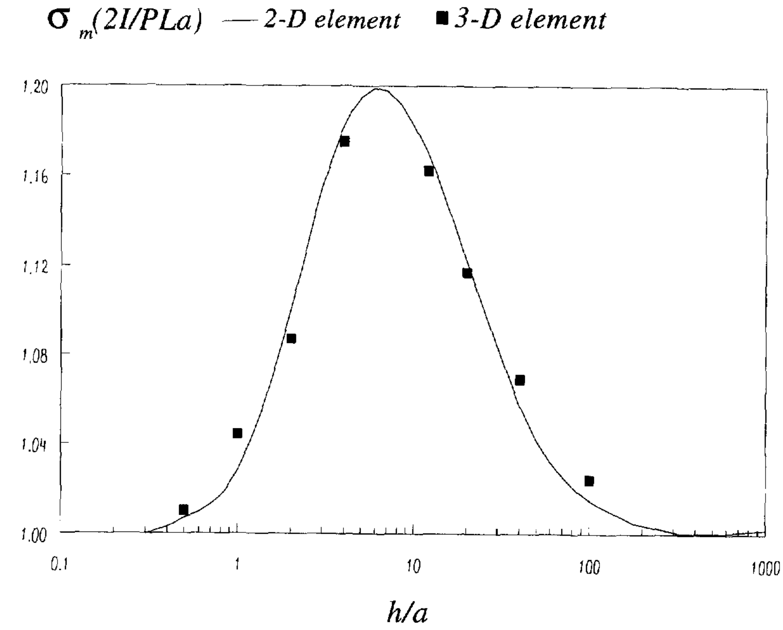

Fig. 3. The influence of thickness on maximum stress.

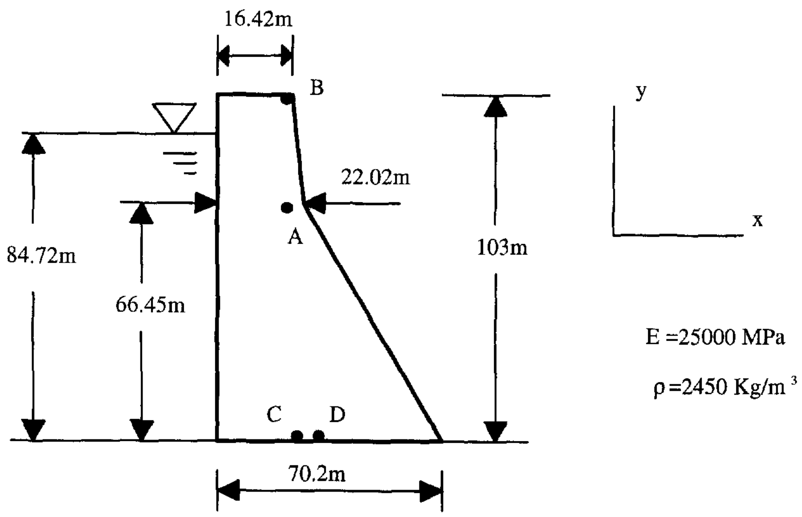

Fig. 4. Koyna dam.

dimensional analysis. Numerical results also show that the lateral stress $\sigma_z \to 0$ as $h \to 0$, while $\varepsilon_z \to 0$ as $h \to \infty$.

From the analysis of the Koyna dam (Ayari (1988)) shown in Fig. 4, the stress components at typical points A, B, C and D of the mid-plane are depicted in Figs 5–8. The dam is subjected to water pressure and gravity. The influence of the thickness can be seen from these figures. Only when the half-thickness is larger than 1000 m, that is, ten times the height of the dam, the plane strain assumption prevails. Marginally, the plane stress state would be admissible in the range of less than 1 m. It is worthy of noting that the lateral tensile stress is larger than the planar tensile stress when the thickness h is larger than a certain value.

The analysis of the same problem has been carried out for different Poisson's ratios. As expected and similar to conventional 3-D analyses, it is found that the influence of the thickness on the stress state is sensitive to Poisson's ratio. When ν is small the discrepancy between plane stress and plane strain states can be less than 5%.

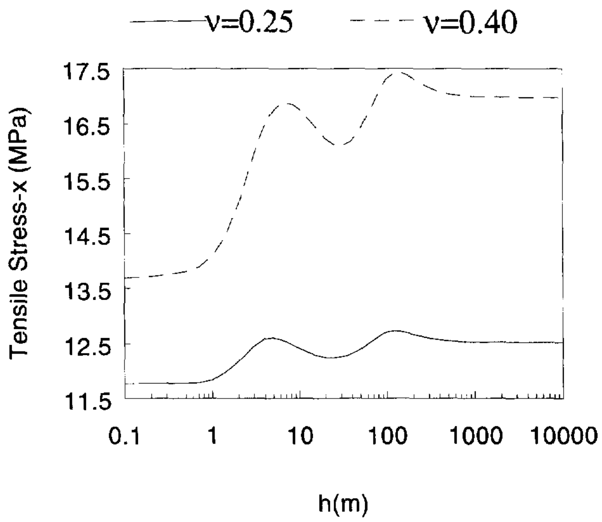

Fig. 5. σ_x at A.

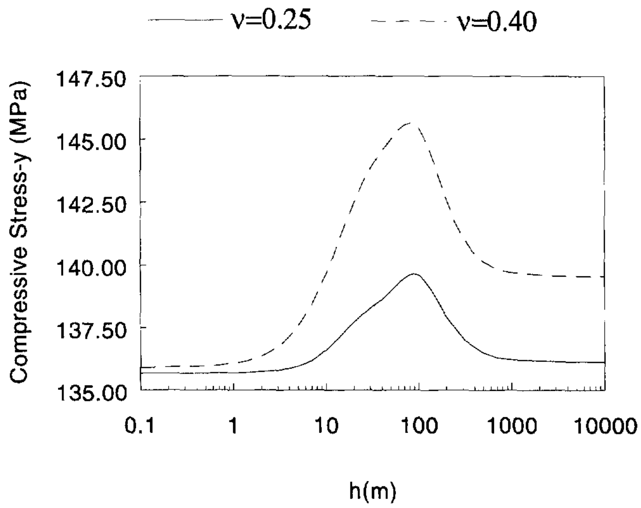

Fig. 6. σ_y at D.

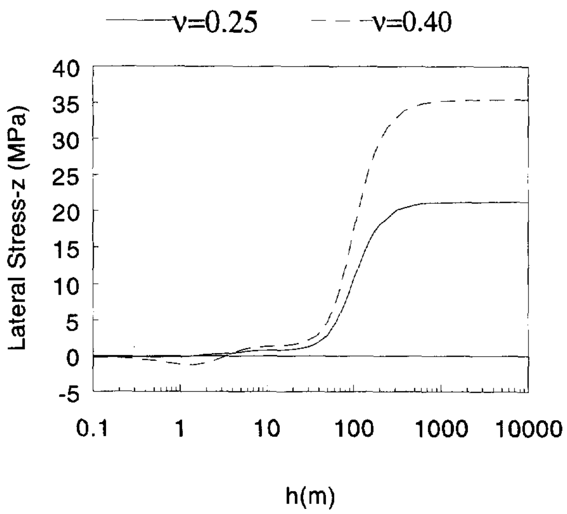

Fig. 7. σ_z at B.

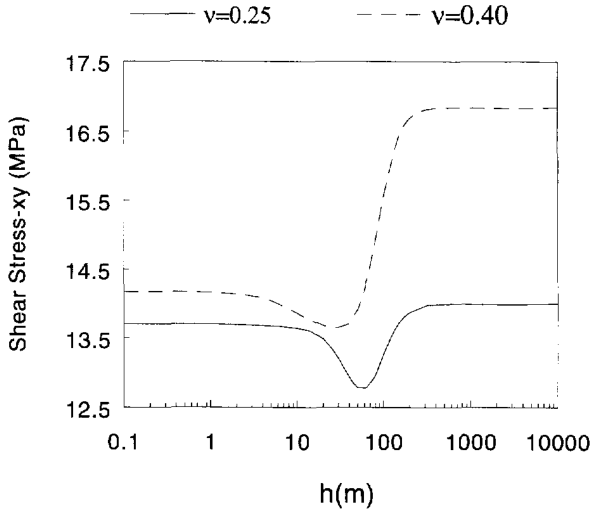

Fig. 8. τ_{xy} at C.

7. DISCUSSION

Because of the out-of-plane displacement mode given by eqn (16), the lateral strain is actually approximated to be constant along the z-direction, and subsequently the free traction condition on the lateral surfaces could not be satisfied. The variational process results in an average lateral strain and stress, which coincides well with 3-D FEM results at mid-planes. Furthermore, the out-of-plane shear stresses given by eqn (17) are automatically introduced into the variational formula as a penalty term ($\mathbf{B}_2^T G \mathbf{B}_2$ in formula (33)), and their magnitudes are therefore made negligible. Their numerical behavior is similar to the secondary stresses occurring in bending problems using conventional finite element analysis. The effect of the terms u_1 and v_1 on the planar stress components is not significant, but they are necessary for the satisfaction of conditions (35) and (36).

Numerical analyses show that for linear elastic materials with the same plane geometry and loading conditions plane stress and plane strain states give different displacements and stresses. The discrepancy can reach about 20% or more. Both examples indicate that for a certain thickness the stress level can be higher than the one predicted by either plane stress or plane strain states. Generally when half the thickness is larger than 100 times the typical planar size, the plane strain state prevails. For many dams built in the form of structurally independent blocks, the block thickness fits the range in which neither plane stress nor plane strain states are suitable for analyses.

In addition, the maximum tensile stress can be the lateral tensile stress rather than the in-plane stress components. For this type of problem, 3-D analysis is computationally expensive. This type of finite element gives an average lateral stress and strain. Conversely, there is one important issue concerning this element. In order to have a solution for an arbitrary thickness, one has to separately store and decompose each one of the three parts of the stiffness matrix. This would lead to a requirement of three times the storage and one reduction plus one back substitution for each thickness. Nevertheless, this element remains quite attractive for planar analyses as it provides solutions which range from plane stress to plane strain ones.

8. CONCLUSION

By relaxing the plane stress condition $\sigma_z = 0$ to a harmonic form, $\nabla^2 \sigma_z = 0$, we obtain a solution which satisfies all the compatibility equations. In this solution the strains consist of one part which is independent of the z coordinate and a second part which includes a z^2 term. Based on this, a set of displacement modes and a new two-dimensional element are proposed for finite element planar stress analyses. Both classic plane stress and plane strain states are retrieved by this new element. The effect of lateral stress σ_z is included in the analysis. We found that σ_z makes the in-plane stress states shift from plane stress to plane strain condition in non-monotonic fashion. Therefore, the assumption of plane stress and plane strain states being a set of bounding solutions may lead to errors. An error of 20% was found in the maximum bending stress of a cantilever beam. This element is attractive because it may eliminate the tedious 3D meshing and data processing in numerous problems. It is also useful for practical design applications, where parametric studies are usually conducted to determine an optimal thickness for structural components. In addition this element can be used as an alternative of classical plane stress and plane strain 2D elements. Finally, further studies are required to establish the embedded energy modes of this element as well as its behaviors around singularities.

Acknowledgement—The financial support for this research provided by Manitoba Hydro, Canada and the National Science and Engineering Research Council of Canada is greatly acknowledged.

REFERENCES

Ayari, L. M. (1988). Static and dynamic fracture mechanics of concrete gravity dams, Ph.D. thesis, University of Colorado at Boulder.

Broek, D. (1982). *Elementary Engineering Fracture Mechanics* (3rd revised ed.), Martinus Nijhoff, Hague.

Fung, Y. C. (1965). *Foundations of Solid Mechanics*, Prentice-Hall Inc.

Love, A. E. H. (1927). *A Treatise on the Mathematical Theory of Elasticity*, 4th ed., Oxford University Press, Oxford, U.K.

Timoshenko, S. and Goodier, J. N. (1954). *Theory of Elasticity*, Oxford University Press, Oxford, U.K.

Zhou, S. & Hsieh, R. (1988). A thickness criterion for fracture toughness testing based on a plane stress compatible solution. *Engng Fract. Mech.* **29**, 41–47.

APPENDIX

According to formula (22) the element stiffness matrix is:

$$\mathbf{K}_e = 2h\int_{\Omega_e}\left[\mathbf{B}_0^{\mathrm{T}}\mathbf{D}_1\mathbf{B}_0 + \frac{h^2}{3}(\mathbf{B}_0^{\mathrm{T}}\mathbf{D}_1\mathbf{B}_1 + \mathbf{B}_1^{\mathrm{T}}\mathbf{D}_1\mathbf{B}_0 + \mathbf{B}_2^{\mathrm{T}}G\mathbf{B}_2) + \frac{h^4}{5}\mathbf{B}_1^{\mathrm{T}}\mathbf{D}_1\mathbf{B}_1\right]\mathrm{d}\Omega \tag{33}$$

The three terms under integration in the above expression are:

$$\mathbf{B}_0^{\mathrm{T}}\mathbf{D}_1\mathbf{B}_0 = [\mathbf{K}_{ij}^1] \quad i,j = 1,\ldots,n,$$

$$[K_{ij}^1] = \frac{E(1-v)}{(1+v)(1-2v)}\begin{bmatrix} N_{i,x}N_{j,x}+v_2N_{i,y}N_{j,y} & v_1N_{i,x}N_{j,y}+v_2N_{i,y}N_{j,x} & v_1N_{i,x}N_j & 0 & 0 \\ v_1N_{i,y}N_{j,x}+v_2N_{i,x}N_{j,y} & N_{i,y}N_{j,y}+v_2N_{i,x}N_{j,x} & v_1N_{i,y}N_j & 0 & 0 \\ v_1N_iN_{j,x} & v_1N_iN_{j,y} & N_iN_j & 0 & 0 \\ 0 & 0 & 0 & 0 & 0 \\ 0 & 0 & 0 & 0 & 0 \end{bmatrix}$$

$$\frac{h^2}{3}(\mathbf{B}_0^{\mathrm{T}}\mathbf{D}_1\mathbf{B}_1 + \mathbf{B}_1^{\mathrm{T}}\mathbf{D}_1\mathbf{B}_0 + \mathbf{B}_2^{\mathrm{T}}G\mathbf{B}_2) = [\mathbf{K}_{ij}^2] \quad i,j = 1,\ldots,n,$$

$$[\mathbf{K}^2_{ij}] = \frac{Eh^2(1-v)}{3(1+v)(1-2v)} \begin{bmatrix} 0 & 0 & 0 & N_{i,x}N_{j,x}+v_2N_{i,y}N_{j,y} & v_1N_{i,x}N_{j,y}+v_2N_{i,y}N_{j,x} \\ 0 & 0 & 0 & v_1N_{i,y}N_{j,x}+v_2N_{i,x}N_{j,y} & N_{i,y}N_{j,y}+v_2N_{i,x}N_{j,x} \\ 0 & 0 & v_2(N_iN_{j,x}+N_{i,y}N_{j,y}) & v_1N_iN_{j,x}+2v_2N_{i,x}N_j & v_1N_iN_{j,y}+2v_2N_iN_{i,y} \\ N_{i,x}N_{j,x}+v_2N_{i,y}N_{j,y} & v_1N_{i,x}N_{j,y}+v_2N_{i,y}N_{j,x} & v_1N_{i,x}N_j+2v_2N_iN_{j,x} & 4v_2N_iN_j & 0 \\ v_1N_{i,y}N_{j,x}+v_2N_{i,x}N_{j,y} & N_{i,y}N_{j,y}+v_2N_{i,x}N_{j,x} & v_1N_{i,y}N_j+2v_2N_iN_{j,y} & 0 & 4v_2N_iN_j \end{bmatrix},$$

$$\frac{h^4}{5}\mathbf{B}_1^T\mathbf{D}_1\mathbf{B}_1 = [\mathbf{K}^3_{ij}] \quad i,j = 1,\ldots,n$$

$$[K^3_{ij}] = \frac{Eh^4(1-v)}{5(1+v)(1-2v)} \begin{bmatrix} 0 & 0 & 0 & 0 & 0 \\ 0 & 0 & 0 & 0 & 0 \\ 0 & 0 & 0 & 0 & 0 \\ 0 & 0 & 0 & N_{i,x}N_{j,x}+v_2N_{i,y}N_{j,y} & v_1N_{i,x}N_{j,y}+v_2N_{i,y}N_{j,x} \\ 0 & 0 & 0 & v_1N_{i,y}N_{j,x}+v_2N_{i,x}N_{j,y} & N_{i,y}N_{j,y}+v_2N_{i,x}N_{j,x} \end{bmatrix},$$

where $(\,)_{,x} = \partial/\partial x$, $(\,)_{,y} = \partial/\partial y$ and n is the number of nodes in an element. And, the stiffness matrix can be written as:

$$K_e = 2h\int_{\Omega_e} [K^1_{ij}+K^2_{ij}+K^3_{ij}]\,\mathrm{d}\Omega \quad i,j = 1,\ldots,n.$$